Atomic Spectroscopy

Article

$MgAl_2O_4$@$MoSe_2$ Nanocomposite for Micro Solid-phase Extraction of Traces Bismuth from Food, Water, and Cosmetic Samples Prior to Quantitation by FAAS

Mustafa Soylak,[a,b,c,*] Abdul Hameed Kori,[a,d] and Hassan Elzain Hassan Ahmed [a,c]

[a] Faculty of Sciences, Department of Chemistry, Erciyes University, 38039 Kayseri, Turkey

[b] Turkish Academy of Sciences (TUBA), Vedat Dalokay Caddesi No: 112, 06670 Cankaya, Ankara, Turkey

[c] Technology Research and Application Center, Erciyes University, 38039 Kayseri, Turkey

[d] National Center of Excellence in Analytical Chemistry, University of Sindh, 67080 Sindh, Pakistan

Received: *October 14, 2023;* ***Revised:*** *November 24, 2023;* ***Accepted:*** *December 25, 2023;* ***Available online:*** *December 25, 2023.*

DOI: 10.46770/AS.2023.264

ABSTRACT: $MgAl_2O_4$@$MoSe_2$ nanocomposite was used to separate-preconcentrate bismuth ions for micro solid phase extraction (μ-SPE). FT-IR, SEM, XRD, SEM-Mapping and SEM-EDX were used to find out about the functional groups, surface morphology, surface area, elemental composition, and crystalline structure of $MgAl_2O_4$@$MoSe_2$. Analytical parameters, such as pH, adsorbent dose, sample volume, eluent concentration and volume, vortex time, and matrix effect, were optimized to get the best recovery values. Under optimized experimental conditions and by using FAAS measurements, analytical parameters were calculated, such as the limit of detection, the limit of quantification, the preconcentration factor, the enhancement factor (EF), the relative standard deviation, the sample volume, and the eluent volume as 0.012 μg L^{-1}, 0.04 μg L^{-1}, 10, 8.69, 5.5, 30 mL, and 3.0 mL, respectively. The validation of the presented procedure was checked by the analysis of certified reference materials and the addition-recovery test to real samples. The presented method was applied for the determination of bismuth contents of natural water, food, and cosmetic products. Two certified reference materials (CRMs) (NCS ZC 73028 Rice and NCS ZC 73036 Green tea) were used for the validation of the presented method.

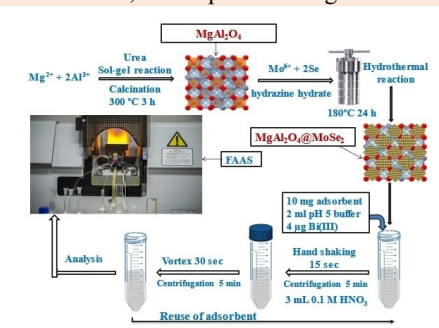

INTRODUCTION

Human activities and industrialization have significantly impacted the environment, leading to the release of metals into water and food chains.[1] Bismuth is found in environmental samples at concentrations ranging from (mg L^{-1} or mg kg^{-1}) to (μg L^{-1} or μg kg^{-1}), and in sediments, concentrations vary from 0.07 to 49.6 mg g^{-1}. [2-4] Bismuth is commonly used in pharmaceuticals for treating stomach ulcers, dermatological issues, and diarrhea.[3] Additionally, it finds applications in cosmetics like body lotions, lipstick, hair dyes, yellow pigments, and certain types of glass.[3,4] Bismuth-based nanomaterials serve various purposes, including semiconductors, alloys, metallurgy additives, and the production of uranium nuclear fuels.[5]

The increasing use of bismuth has led to its widespread distribution in the environment, raising the potential for exposure in organisms. While bismuth is generally considered to have low toxicity for humans and has been employed in medical treatments, chronic exposure can result in adverse effects like osteoarthropathy, hepatitis, neuropathology, encephalopathy, and nephrotoxicity.[6] Consequently, researchers have focused on determining bismuth concentrations in food, water, and environmental samples, even at very low levels. However, the limited presence of bismuth in these samples and the impact of matrix effects have posed challenges in accurate measurement.[7,8]

Various techniques are used to separate and preconcentrate trace inorganic species, including liquid-phase extraction (LPE), solid-

phase extraction (SPE), co-precipitation (CE), and cloud point extraction (CPE).[9,10] Micro solid-phase extraction (μ-SPE) stands out due to its advantages such as high preconcentration, minimal adsorbent use, rapid processes, automation suitability, and use of environmentally friendly chemicals.[11]

Numerous analytical methods have been utilized for bismuth detection in the environment, including flame atomic absorption spectrometry (FAAS), inductively coupled plasma-mass spectrometry (ICP-MS), graphite furnace atomic absorption spectrometry (GF-AAS), ultraviolet-visible spectroscopy (UV-VIS), energy-dispersive x-ray fluorescence spectrometry (ED-XRF), hydride generation for atomic fluorescence spectrometric (HG-AFS), and inductively coupled plasma-atomic emission spectroscopy (ICP-AES).[12-17] FAAS, being easy to use and cost-effective, is prevalent in laboratories.[18-20] However, detecting trace analytes with FAAS is hindered by higher quantification limits and matrix effects. [21,22] Consequently, a separation-preconcentration approach enhancing sensitivity and selectivity is crucial before employing FAAS.[23-26]

Nano porous materials have attracted a great deal of attention compared with other porous materials due to their easily accessible starting materials, low cost, biodegradability, functionalization ability, environmentally friendly nature, high chemical, and mechanical stability, safe, and recyclable. These have wide applications such as energy storage, dye degradation, organic pollutant degradation, water treatment, drug delivery, supercapacitors, fuel cells, nano-reactors, catalysis, dye-sensitized solar cells, and sensors.[27-28] Therefore, recent μ-SPE studies have increasingly adopted new-generation adsorbents.[29] To enhance analytical qualities in micro solid phase extraction (μ-SPE), diverse materials have been utilized, including ion imprinted polymers,[30] graphene oxide or magnetic graphene oxide,[31] nanoparticles,[32,33] silica nanoparticles (SiNPs),[34] cellulose-based magnetic nanoparticles, and carbon nanomaterials (CNMs).[35] $MgAl_2O_4$ nanoparticles have a large surface area and can bind to a variety of chemicals strongly. They are also heat-resistant and can be reused many times. These properties make them very effective at adsorption of trace amounts of metal ions and removing pollutants from water and air. Additionally, $MgAl_2O_4$ nanoparticles can be used as catalysts or to support other functional materials. When $MoSe_2$ is used as a sorbent alone, its efficiency may be limited by its surface area or lack of synergistic interactions with specific analytes.[36,37] The combination of spinel oxides like $MgAl_2O_4$ with molybdenum selenide ($MoSe_2$) nanoparticles holds significant importance and offers a range of promising applications across different fields of science and technology. These nanocomposites offer enhanced properties and tunability, enabling customization for specific applications. With multifunctionality, their potential applications across catalysis, energy storage, sensing, biomedical applications, and environmental extraction and remediation.[37-39]

The adsorption of Bi(III) ions onto an anti-site surface within a spinel structure ($MgAl_2O_4$) is determined by several factors. These factors include ionic charge, the electronic environment around the adsorption site, steric effects, and the potential for chemical bonding. These factors collectively influence the characteristics of the adsorption interaction. The surface of $MgAl_2O_4$ is attracted to water molecules because it is hydrophilic. This attraction can help to improve the adsorption of Bi(III) ions, which are also hydrophilic. The adsorption of Bi(III) ions onto $MoSe_2$ is a complex process that is influenced by a number of factors. The hydrophilic nature of both Bi(III) and $MoSe_2$ likely plays a role in the adsorption process. Chemical bonding, specifically chemisorption, is the main driving force behind the adsorption of Bi(III) onto $MoSe_2$. Further investigation of the interaction between Bi(III) and $MoSe_2$ can be carried out using adsorption isotherm experiments.[40,41]

This research has focused on the formulation of a solid phase extraction (SPE) technique employing $MgAl_2O_4$@$MoSe_2$ nanocomposite for the purpose of effectively separating and pre-concentrating Bi(III) from natural water and food samples as well as digested cosmetic products.

MATERIALS AND METHODS

Reagents and solutions. All chemicals used throughout the study were of analytical purity purchased from Merck (Darmstadt, Germany). Distilled water was supplied from (Millipore, Bedford, MA, USA). Bismuth standard solution of 1000 mg L^{-1} was used as a stock solution throughout the study. Standard solution of Bi(III), magnesium nitrate, aluminum nitrate nonahydrate, urea, sodium molybdate dihydrate, selenium, hydrazine hydrate, ethanol, and nitric acid were obtained from Sigma-Aldrich (St. Louis, MO, USA). The certified reference materials (NCS ZC 73028 Rice and NCS ZC 73036 Green tea) were purchased from the Approved by China National Analysis Center for Iron and Steel (Beijing, China). Phosphate and acetate buffer solutions were used for pH adjustments. Food and cosmetic product samples were purchased from Kayseri markets, Turkey.

Apparatus. A ContrAA 800 (Analytik Jena, Jena, Germany) flame atomic absorption spectrometer was used with an air-acetylene gas mixture with a continuous source for the optimization stages and the measurements of Bi. The fuel and oxidant flow rates were 55 and 500 L/h. A WTW 3110 model digital pH meter (WTW GmbH, Germany) with a glass electrode was used for pH measurements and adjustments. Vortex (Weightlab WN-V 2800 Istanbul, Turkey) was used for the adsorption and desorption processes. A Fourier transform infrared spectrophotometer (Nicolet 5700, Thermofisher, USA) was used for determining functional group spectra. A scanning electron

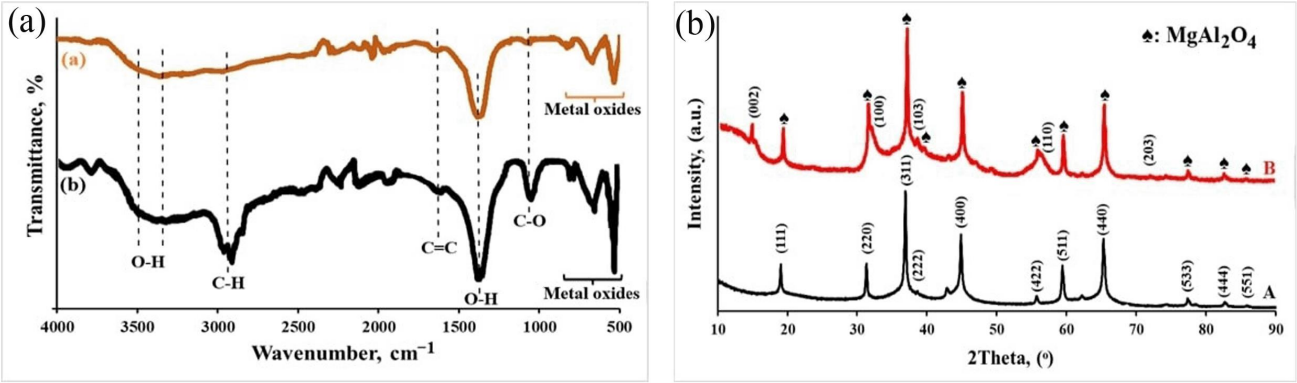

Fig. 1 Schematic presentation of the presented μSPE method of Bi(III).

microscope (SEM, Oberkochen, Germany) was used to observe the morphological structure of the substance. The XRD of the material was performed by a Bruker AXS D8 advanced X-ray powder diffractometer. X-ray diffraction (XRD) analysis was used to illuminate the crystal structure of the synthesized new substance. A compact closed vessel microwave digestion system (Ethos Lean -1, Milestone, Bergamo, Italy) has been used for the digestion of food and cosmetic samples.

Synthesis of $MgAl_2O_4$@$MoSe_2$ nanocomposite. $MgAl_2O_4$ nanoparticles were prepared by adding 0.45 g of magnesium nitrate and 2.31 g of aluminum nitrate nonahydrate, in stoichiometric molar proportions, to 200 mL of deionized water. 1.65 g of urea was added to the resulting solution, and the mixture was stirred at 25 °C for 45 min using a hotplate magnetic stirrer. Subsequently, the temperature of the mixture was elevated to 80 °C until the formation of a transparent gel. The resulting gel was placed in a furnace and heated to 300 °C for a duration of 3 h, leading to the production of $MgAl_2O_4$ nanoparticles. The product was white colored and powder but not fine. The mortar was used to make it fine powder.[36]

To synthesize $MgAl_2O_4$@$MoSe_2$ nanocomposite, a mixture of 1.0 g of sodium molybdate dihydrate and 0.75 g of $MgAl_2O_4$ nanoparticles was combined with a solution containing 20 ml of deionized water and 30 ml of ethanol, resulting in the creation of solution A. Similarly, 0.66 g of selenium powder was dissolved in 15 ml of hydrazine hydrate, leading to the formation of suspension B, which promptly changed color from colorless to very dark violet. The two reaction solutions, A and B, were stirred continuously and then introduced into a 100 ml Teflon-lined stainless-steel autoclave. After being allowed to age at a temperature of 180°C for a duration of 24 h, the autoclave was naturally cooled down to room temperature. The resulting black precipitate was separated through centrifugation and underwent multiple washes with ethanol and deionized water. Subsequently, the obtained product was dried at 80°C for 12 h.[42] Fig. 1 shows the schematic presentation of the synthesis of the nanocomposite and the presented μSPE method of Bi(III).

Analytical procedure. A 30 mL model solution was adjusted to pH 5 using the acetate buffer solution. 200 μL from 20 ppm stock solution of Bi(III) was added to the model solution. 10 mg of $MgAl_2O_4$@$MoSe_2$ was added, hand-shaken for 15 s and centrifuged for 5 min. Then 3 mL of 0.1 M HNO_3 was added for elution and vortexed for 30 seconds and centrifuged for 5 minutes. The decanted solution was collected for FAAS for bismuth determination.

Preparation of food and cosmetic samples. For digestion, approximately 250 mg each food and cosmetic samples were digested with 5 mL of HNO_3 and 1 mL of H_2O_2 in PTFE vessels. The digestion was carried out by setting the manufacture protocol. After cooling down to room temperature, digested samples were taken out, and neutralized their pH according to our required method for further treatment.[43]

Application of developed method to real samples. The developed μ-SPE method was used for the solid micro phase extraction for selection the of the selected target analyte from natural water samples (Tap, lake, and industrial wastewater samples). Natural water samples were subjected to centrifugation to remove solid suspended particles. The developed method was applied to determine Bi(III) levels.

For the digested subsamples of food, cosmetics, and CRMs (NCS ZC 73028 Rice and NCS ZC 73036 Green tea). A 0.25 g of the sample were placed in a polytetrafluoroethylene (PTFE) vessel along with 5 mL of nitric acid and 1 mL of hydrogen peroxide. The vessels were sealed and heated according to a two-stage digestion protocol: an initial 5-minute ramp to 180°C followed by a 10-minute hold at 180°C.[44] Upon cooling, the digested sample solutions were transferred to 50-milliliter centrifuge tubes, and the pH was adjusted to near 7. Certain volumes were taken from digested food, cosmetics and CRMs and the developed method

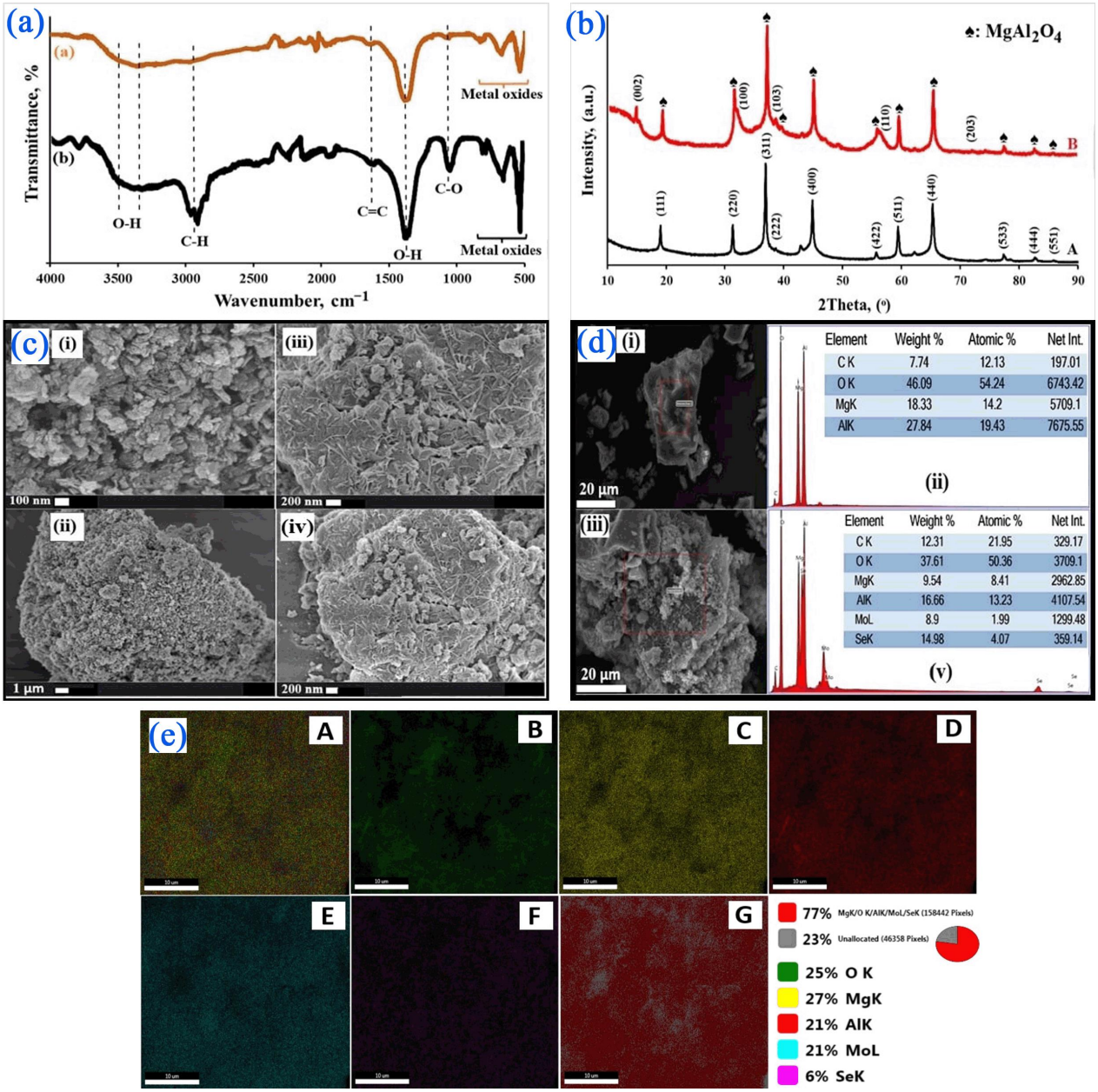

Fig. 2 (a): IR spectra of $MgAl_2O_4$ (a) and $MgAl_2O_4$@$MoSe_2$ (b); (b): XRD patterns of $MgAl_2O_4$ (A) and $MgAl_2O_4$@$MoSe_2$ (B); (c): SEM images of $MgAl_2O_4$ (i and ii) and $MgAl_2O_4$@$MoSe_2$ (iii and iv); (d): SEM-EDX of $MgAl_2O_4$ (i and ii) and $MgAl_2O_4$@$MoSe_2$ (iii and iv); (e): SEM-Mapping image of $MgAl_2O_4$@$MoSe_2$, element percentages (A), oxygen (B), magnesium (C), aluminum (D), molybdenum (E), selenium (F), and all elements (G).

was applied to determine Bi(III) levels. Standard addition and direct analysis of the analyte were performed in this work.

RESULTS AND DISCUSSION

Characterization of $MgAl_2O_4$@$MoSe_2$ nanocomposite. $MgAl_2O_4$ was synthesized through the sol-gel method for utilization as a substrate for nanocomposites. Subsequently, a fine layer of $MoSe_2$ was applied onto it. The resultant nanocomposite underwent comprehensive analysis using various methodologies. The Fourier-transform infrared (FT-IR) spectra of the synthesized product recorded in the range 400 - 4000 cm^{-1} are depicted in Fig. 2a. Within the IR spectra (Fig. 2a (a)), the $MgAl_2O_4$ samples exhibited three distinct vibrations at wavenumbers 530, 635, and 760 cm^{-1}, signifying the presence of AlO_6 moieties, the lattice vibration corresponding to Mg-O stretching, and confirming the formation of the $MgAl_2O_4$ spinel structure. Particularly noteworthy were two vibrational bands at wavenumbers 3456 and

1401 cm^{-1} within the IR spectra of the products, likely originating from the stretching and bending vibrations of water molecules adsorbed on the $MgAl_2O_4$ substrate.[45,46] In the spectrum of $MgAl_2O_4$@$MoSe_2$ (Fig. 2a (b)), the peaks observed at 520, 635, and 771 cm^{-1} correspond to the bands of metal oxides (Mg-O & Al-O). The signals at 3450 and 2903 cm^{-1} can be linked to the stretching vibrations of Mo-Se and hydroxyl groups within the $MgAl_2O_4$@$MoSe_2$ nanocomposite.[47,48]

Figure 2b displays the XRD diagrams of $MgAl_2O_4$ and $MgAl_2O_4$@$MoSe_2$. The distinctive diffraction peaks attributed to the Bragg reflections from planes like (111), (220), (311), (222), (400), (422), (511), (440), (533), (444), and (551) aligned with the well-known standard spinel arrangement of $MgAl_2O_4$ (as per JCPDS Card No. 01-075 1798), depicted in Fig. 2b (A).[46] In Fig. 2b (B), the XRD graph presents peaks for the $MgAl_2O_4$@$MoSe_2$ nanocomposite. The specific peaks located at angles of 2θ = 14.54°, 31.82°, 38.38°, 56.16°, and 71.97°, which match the planes (002), (100), (103), (110), and (203) respectively, are associated with MoSe2 (according to JCPDF 29-0914). The remaining peaks marked with the (♠) symbol correspond to $MgAl_2O_4$. [49]

SEM and SEM-EDX were employed to investigate the morphology of the synthesized nanocomposite. The SEM images of $MgAl_2O_4$ can be observed in Figs. 2c (i) and (ii). These images display that $MgAl_2O_4$ is well dispersed and most of the prepared nanoparticles have shapes at the nanoscale.[46] SEM images of $MgAl_2O_4$@$MoSe_2$ are presented in Figs. 2c (iii) and (iv). As illustrated in Fig. 2c (iii), $MgAl_2O_4$@$MoSe_2$ is observed in clusters of nanoparticles, made up of thin layers. This observation indicates the successful doping of $MoSe_2$ onto the surface of $MgAl_2O_4$.[50] The EDX analysis is displayed in Figs. 2d (i)-(iv). This analysis clearly demonstrates the existence of all the anticipated primary elements (O, Mg, and Al in the case of $MgAl_2O_4$) and (O, Mg, Al, Mo, and Se in the case of $MgAl_2O_4$@$MoSe_2$), which encompass the two specified nanoparticles.

The SEM-Mapping image of $MgAl_2O_4$@$MoSe_2$ in Fig 2e (A-G) shows that the nanoparticles were successfully synthesized.

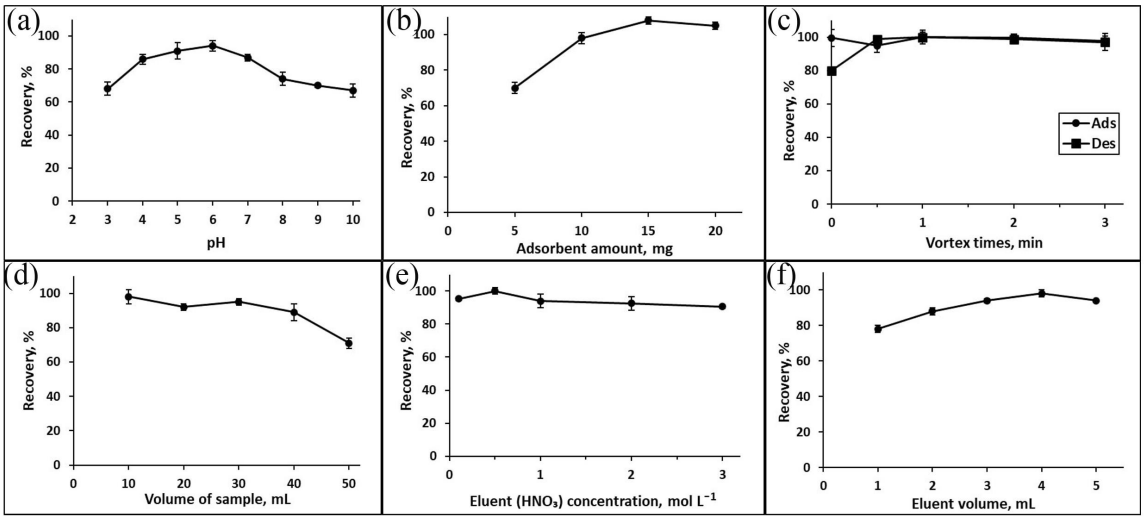

Fig. 3 (a): Effect of pH on the recoveries of Bi(III), (N= 3); 200 µL from (20 mg L^{-1}) Bi(III); Buffer solution: 2 mL, pH 3 - 10; Adsorbent amount: 15.0 mg; Vortex time for sorption: 2 min; Centrifuge time for sorption: 5 min; Vortex time for desorption: 2 min; Centrifuge time for desorption: 5 min; Sample volume: 10 mL; Eluent volume: 5 mL; Eluent: 3 mol L^{-1} of HNO_3, (N = 3). (b): Effect of adsorbent amount on the recoveries of Bi(III), (N= 3); 200 µL from (20 mg L^{-1}) Bi(III); Buffer solution: 2 mL, pH 5; Adsorbent amount: 5.0 – 20.0 mg; Vortex time for sorption: 2 min; Centrifuge time for sorption: 5 min; Vortex time for desorption: 2 min; Centrifuge time for desorption: 5 min; Sample volume: 10 mL; Eluent volume: 5 mL; Eluent: 3 mol L^{-1} of HNO_3, (N = 3). (c): Effect of adsorption and desorption vortex time (N=3); 200 µL from (20 mg L^{-1}) Bi(III); Buffer solution: 2 mL, pH 5; Adsorbent amount: 10.0 mg; Vortex time for sorption: 0 – 3.0 min; Centrifuge time for sorption: 5 min; Vortex time for desorption: 2 min; Centrifuge time for desorption5 min; Sample volume: 10 mL; Eluent volume: 5 mL; Eluent: 3 mol L^{-1} of HNO_3, (N = 3). 200 µL from (20 mg L^{-1}) Bi(III); Buffer solution: 2 mL, pH 5; Adsorbent amount: 10.0 mg; Vortex time for sorption: 15 sec; Centrifuge time for sorption: 5 min; Vortex time for desorption: 0 – 3.0 min; Centrifuge time for desorption: 5 min; Sample volume: 10 mL; Eluent volume: 5 mL; Eluent: 3 mol L^{-1} of HNO_3, (N = 3). (d): Effect of sample volume (N=3); 200 µL from (20 mg L^{-1}) Bi(III); Buffer solution: 2 mL, pH 5; Adsorbent amount: 10.0 mg; Vortex time for sorption: 15 sec; Centrifuge time for sorption: 5 min; Vortex time for desorption: 0 – 3.0 min; Centrifuge time for desorption: 5 min; Sample volume: 10 - 50 mL; Eluent volume: 5 mL; Eluent: 3 mol L^{-1} of HNO_3, (N = 3). (e): Effect of eluent concentration (N=3); 200 µL from (20 mg L^{-1}) Bi(III); Buffer solution: 2 mL, pH 5; Adsorbent amount: 10.0 mg; Vortex time for sorption: 15 sec; Centrifuge time for sorption: 5 min; Vortex time for desorption: 0 – 3.0 min; Centrifuge time for desorption: 5 min; Sample volume: 30 mL; Eluent volume: 1.0 – 5.0 mL; Eluent: 3 mol L^{-1} of HNO_3, (N = 3). (f): Effect of eluent volume (N=3); 200 µL from (20 mg L^{-1}) Bi(III); Buffer solution: 2 mL, pH 5; Adsorbent amount: 10.0 mg; Vortex time for sorption: 15 sec; Centrifuge time for sorption: 5 min; Vortex time for desorption: 0 – 3.0 min; Centrifuge time for desorption: 5 min; Sample volume: 30 mL; Eluent volume: 3.0 mL; Eluent: 0.1 – 3.0 mol L^{-1} of HNO_3, (N = 3).

The elements are uniformly distributed, with Mg and Al concentrated in the core and Mo and Se concentrated in the shell. This suggests that the $MgAl_2O_4$@$MoSe_2$ core-shell nanoparticles have a cubic structure with Mg and Al atoms occupying the tetrahedral and octahedral sites, respectively. The Mo atoms are sandwiched between two layers of Se atoms in a hexagonal structure.

Method optimization

Effect of pH on adsorption process. pH is one of the most important factors that affect the adsorption efficiency of the adsorbent.[51] In situations where a ligand is absent during the metal sorption process, the role of pH in influencing the results becomes more noticeable. The acidity or alkalinity of the solution directly affects how soluble the metal ions are and the types of chemical structures they take. In an acidic media, the metal ions usually exist as independent, hydrated forms, whereas in a basic solution, they tend to create hydroxide complexes or solid particles.[52,53] The effect of pH on the adsorption of Bi(III) on $MgAl_2O_4$@$MoSe_2$ was investigated in the range of 3 − 10 as shown in Fig. 3a. It can be concluded from Fig. 3a, that the % recoveries of Bi(III) increases as pH of the solution increases from 2 to 5. There is a substantial decrease in % recovery of the metals above pH 5. It can be explained that at higher pH, there is a high concentration of OH^- ion, and most of the vacant sites on the surface of the adsorbent were occupied by OH^- and thus decreased the % recovery of the metal ions. Therefore, pH 5 was the optimum pH which was maintained in other optimization experiments.

Adsorbent amount study. The amount of the adsorbent is also another critical parameter for the quantitative recoveries of the analytes in the solid phase extraction studies.[54] The adsorption of Bi(III) ions onto $MgAl_2O_4$ and $MoSe_2$ is driven by a combination of electrostatic and chemical interactions. The hydrophilic nature of $MgAl_2O_4$ facilitates the adsorption of Bi(III) ions, while chemisorption is the primary driving force for Bi(III) binding onto $MoSe_2$. The specific type of chemical bond that forms between Bi(III) and $MoSe_2$ depends on the pH of the solution and the presence of other ions. Adsorption isotherm experiments can be used to further investigate the nature of the interaction between Bi(III) and these two sorbents.[55,56] The recovery values of Bi(III) are dependent on the amount of adsorbent. To explore the impact of $MgAl_2O_4$@$MoSe_2$ quantity, preconcentration experiments were conducted using dosages ranging from 5 mg to 20 mg (Fig. 3b). Results indicate that the % recoveries of Bi(III) were enhanced, as the amount of adsorbent amount increased, and quantitative recoveries of Bi(III) were found at 10 − 20 mg as shown in Fig. 3b. Adsorbent has a higher surface area and porosity, so it adsorbs more metal ions. Hence, 10 mg was chosen as the optimal amount of adsorbent for further studied.

Vortex time. During the process of micro solid-phase extraction, the adsorption of target analytes onto the surface of the solid phase occurs through mechanisms encompassing van der Waals forces, hydrogen bonding, and specific chemical interactions. The temporal extent of adsorption significantly influences the quantity of analytes sequestered by the solid phase, a parameter subject to modulation by various factors including the inherent characteristics of the analytes, the properties inherent to the solid phase, and the composition of the sample matrix.[53] To obtain the maximum efficiency of absorption and desorption of Bi(III) over adsorbent the preconcentration studies were conducted at different vortex times ranging from hand shaking to 3 min as shown in Fig. 3c. The outcomes show that quantitative adsorption and quantitative desorption were obtained in hand shaking (15 sec) and 30 sec respectively. Further increase in vortex time has no significant effect on adsorption process and recovery values of Bi(III). It can also be concluded from the results that after the further work was established in hand shaking for adsorption and 30 sec for desorption.

Table 1. Effect of some foreign ions on the recoveries of 200 µL from (20 mg L^{-1}) Bi(III) (N= 3)

Ions	Added as	Concentration, mg L^-	Recovery, %
Na^+	$NaNO_3$	2000	94 ± 0[a]
K^+	KNO_3	2500	101 ± 2
Ca^{2+}	$CaCO_3$	250	90 ± 4
Mg^{2+}	$Mg(NO_3)_2.6H_2O$	250	107 ± 3
Fe^{2+}	$FeCl_2$	5.0	95 ± 1
Zn^{2+}	$Zn(NO_3)_2.6H_2O$	2.5	91 ± 3
Fe^{3+}	$Fe(NO_3)_3.9H_2O$	2.0	97 ± 3
Al^{3+}	$Al(NO_3)_3.9H_2O$	100	102 ± 4
Mn^{2+}	$Mn(NO_3)_2.4H_2O$	2.5	91 ± 0
Cl^-	KCl	2000	99 ± 4
SO_4^{2-}	Na_2SO_4	250	97 ± 3
CO_3^{2-}	$CaCO_3$	375	90 ± 4
NO_3^-	$NaNO_3$	4500	94 ± 0
HPO_4^{3-}	Na_2HPO_4	500	96 ± 1

[a] Mean ± Standard deviation

Sample volume and desorption studies. The sample volume plays an important role in µ-SPE for achieving the highest preconcentration factor.[53] Fig. 3d shows the relationship between the sample volume and recovery of Bi(III) ions. Sample volume was tested in the range of 10 – 50 mL. There is a quantitative recovery at the volume rnage of 10 – 30 mL. The obtimal sample volume was chosen as 30 mL and has been used in the rest experiments.

Desorption of Bi(III) from $MgAl_2O_4$@$MoSe_2$ was carried out using diluted solutions of mineral acids like HCl and HNO_3. HNO_3 may be better than HCl for analytes that form stable and soluble complexes with nitrates, making it an optimal choice for their elution. It minimizes the risk of chloride interference (when HCl is used), which is particularly important when analyzing metals. For this reason, desorption studies were carried out using 0.1 to 3 M HNO_3 solutions for the quantitative recovery of Bi(III). The recovery results are given in Fig. 3e, showing that quantitative recoveries of Bi(III) can be obtained using 0.1 M HNO_3. For

Table 2. Study of Bi(III) levels in natural water, food, and cosmetic product samples, (N = 3)

Samples		Added, μg mL^{-1}	Found, μg mL^{-1}	Recovery, %	%RSD (N = 3)
Water	Talas tap water	0.000	ND	---	---
		0.150	0.143 ± 0.005[a]	95	3.2
		0.300	0.278 ± 0.010	93	3.9
	Kocasinan tap water	0.000	ND	---	---
		0.150	0.139 ± 0.002	93	1.5
		0.300	0.288 ± 0.009	96	3.0
	Incesu tap water	0.000	ND	---	---
		0.150	0.133 ± 0.007	87	5.0
		0.300	0.275 ± 0.011	92	4.1
Food	Dried chickpea	0.000	ND	---	---
		0.250	0.214 ± 0.008	86	3.5
		0.500	0.454 ± 0.015	91	3.4
	Red lentil	0.000	0.009 ± 0.000	---	4.6
		0.250	0.247 ± 0.002	95	0.9
		0.400	0.382 ± 0.006	93	1.5
	Dry sweet corn	0.000	ND	---	---
		0.250	0.255 ± 0.005	102	1.9
		0.500	0.480 ± 0.022	96	4.5
	Chicken liver	0.000	ND	---	---
		0.200	0.191 ± 0.006	96	2.9
		0.400	0.368 ± 0.015	92	4.1
	Beef liver	0.000	ND	---	---
		0.200	0.183 ± 0.010	92	5.5
		0.400	0.359 ± 0.018	90	5.1
Cosmetic	Nivea body cream	0.000	0.015 ± 0.001	---	3.9
		0.200	0.201 ± 0.009	93	4.5
		0.400	0.395 ± 0.013	95	3.3
	Neutrogena body cream	0.000	0.104 ± 0.004	---	3.5
		0.200	0.290 ± 0.006	93	2.0
		0.400	0.488 ± 0.010	96	2.1
	Arko body cream	0.000	ND	---	---
		0.200	0.182 ± 0.009	91	5.1
		0.400	0.351 ± 0.014	88	3.9

ND: No detection; [a] Mean ± Standard deviation.

eluent volume, desorption studies were conducted at different volumes of 0.1 M HNO_3, ranging from 0.5 - 5 mL (Fig. 3f). It can be concluded from the Fig. 3e that 3 mL of 0.1 M HNO_3 was enough to obtain quantitative recoveries Bi(III) using $MgAl_2O_4$@$MoSe_2$.

Matrix effects. For the selectivity of the method, studying the effect of different ions which are coexisting with the analyte metals in sample matrices is of immense importance.[57-64] Distinct cations and anions, including were individually introduced into the model solutions to assess the method as described earlier. The effect of different ions, which are coexisting with analyte ions was studied on the percent recovery of Bi(III). The quantitative recovery results are given in Table 1 and show that there is no significant matrix effect on the % recovery of analyte ions. Based on the study findings, the analysis remained unaffected by the existence of Fe(II), Fe(III), Zn(II), and Mn(II) ions at concentrations ranging from 6 to 12 times higher than that of the target metal ion. The addition of foreign ions K^+, Na^+, Al^{3+}, Mg^{2+}, Ca^{2+}, SO_4^{2-}, NO_3^-, Cl^-, HPO_4^{2-} and CO_3^{2-} at concentrations up to 6500 mg L^{-1} did not affect the recovery of Bi(III) from aqueous solutions. This suggests that these ions do not have a significant effect on the adsorption of Bi(III) onto the adsorbent. It can be concluded from the matrix effect that the method is highly selective for the preconcentration of Bi(III).

Analytical performance. The limit of detection (LOD), limit of quantification (LOQ), and preconcentration factor of the developed method were evaluated. To establish the calibration relationship, standard solutions were prepared, and their absorbance values were measured. The preconcentration factor (PF) was determined as the average of measurements of the model solution volume divided by the final volume after extraction. The LOD was determined using a calculation based the ratio of 3 s/m, where (s) represents the standard deviation of the blank absorbance (N = 10) and (m) represents the slope of the calibration curve. Similarly, the limit of quantitation (LOQ) was calculated using the relation of 10 s/m. The LOD, LOQ, R^2, PF, enhancement factor (EF), and RSD% were obtained as 0.012 μg L^{-1},0.04 μg L^{-1}, 0.997, 10, 8.69, and 5.5, respectively.

Application to real samples. The method was validated by the

Table 3. Levels of Bi(III) in CRMs after application of presented µSPE method, (N = 3)

Certified Reference Material (CRM)	Certified value, µg kg^{-1}	Observed value, µg kg^{-1}	Recovery, %	Relative error (%)
NCS ZC 73028 Rice	16	14.4 ± 2.11	90	-11
NCS ZC 73036 Green tea	40.0 ± 11.0	36.0 ± 4.7	91	-11

Table 4. Comparison of separation-preconcentration studies with µSPE for Bi(III)

Adsorbent	Detection system	LOQ, µg L^{-1}	PF	Linear range, µg L^{-1}	RSD, %	Ref.
Octadecyl bonded silica cartridge modified with cyanex 301	ETAAS	0.033	20	0.5–10	---	56
Chitosan functionalized with 3,4-dihydroxy benzoic acid	ICP-AES	0.233	8.4	0–5	0.5–4	57
Quinolin-8-ol and Amberlite XAD-7	HG-ICP-OES	0.067	37	DL-100	3.5	7
2-(5-bromo-2-pyridylazo)-5-diethylaminophenol	ETAAS	0.029	300	0.035–0.35	4.1	65
2-(5-bromo-2-pyridylazo)-5-diethylaminophenol complex on amberlite XAD-2	Voltammetry	0.467	---	50–160,000	1.2	66
Rice Husk	FAAS	4.333	40	---	1.8	67
Amberlite XAD-16	FAAS	900 µg kg^{-1}	30	---	<12	68
TiO_2 nanoparticles	TS-FF-AAS	1.13	67	Upper linear range 0.15 mg L^{-1}	3.7	69
$MgAl_2O_4$@$MoSe_2$	FAAS	0.04	10	0.2 - 100	5.5	Present work

Note: ETAAS: Electrothermal atomic absorption spectrometry, FAAS: Flame atomic absorption spectrometry, LOQ: Limit of quantification, PF: Preconcentration factor, HG-ICP-OES: Hydride generation inductively coupled plasma atomic emission spectrometry, TS-FF-AAS: Thermospray flame furnace atomic absorption spectrometry.

standard addition recovery method and certified reference material. Different natural water samples were used in the standard addition recovery studies (Table 2). The validated method was also employed to determine bismuth content in some food, and cosmetic product samples from local markets in Kayseri (Table 2). The certified reference materials (NCS ZC 73028 Rice and NCS ZC 73036 Green tea) were also used to validate the method (Table 3). There is an agreement between the measured results and the certified values. The recovery of Bi(III) from both rice and green tea CRMs was around 90%. This indicates that the µSPE method is effective at recovering Bi(III) from these materials. The developed method was compared to previously reported methods as shown in Table 4. The advantages of this method can be summarized as a low LOD and LOQ, a wide linear range (0.2 – 100 µg L^{-1}), and reasonable precision. While it may not achieve the highest preconcentration factor when compared to other methods, it strikes a balance between sensitivity, versatility, and reliability, making it a valuable addition to the range of preconcentration techniques available for the analysis of Bi(III) in different sample matrices. This innovation enhances the tools accessible for trace metal analysis, offering an effective and adaptable approach for researchers and analysts and it is a very competitive technique by comparison with other costly approaches.

CONCLUSION

A novel material known as $MgAl_2O_4$@$MoSe_2$ was successfully synthesized to use as a solid-phase extracting material for the separation-preconcentration of bismuth ions Bi(III) from some cosmetic products, natural water, and food samples. This choice of material was based on its advantageous characteristics, including a larger surface area and bigger pores, which enhance its adsorptive capacity to adsorb heavy metal ions effectively. To comprehensively characterize the newly synthesized material, a range of analytical techniques were employed. The methodology proved to be robust, cost-effective, selective, and sensitive in the detection of Bi(III) ions in environmental and cosmetic product samples. In conclusion, the synthesized $MgAl_2O_4$@$MoSe_2$ material exhibited its potential as a solid-phase extracting agent for efficient preconcentration of Bi(III) ions from complex environmental and food samples. The multi-technique characterization and thorough analytical validation collectively underscore the feasibility and applicability of the proposed method, offering a valuable tool for accurate detection of Bi(III) in diverse sample matrices.

AUTHOR INFORMATION

Prof. Mustafa Soylak is working on Environmental Analytical Chemistry, Nanotechnology, Nanomaterials, Nanocomposites, Separation/ Preconcentration Techniques including Solid Phase Extraction, Coprecipitation, Cloud point extraction, membrane filtration, speciation and microextraction of trace organic and inorganic species. Dr. Soylak has an h-index of 112 (Web of science). He has over 750 papers in Web of Science, 8 book chapters and reviews, two textbooks (in Turkish), one textbook on microextraction techniques (Elsevier, 2020). He is Editor-in-Chief of Comprehensive Sampling and Sample Preparation (Elsevier, 2023). He was visiting professor at King Saud University- Saudi Arabia on 2010-2016 and at Near East University-Cyprus on 2018-2019. He is now Professor at Erciyes University, Department of Chemistry, Kayseri-Turkey. He is the editorial board member of *Atomic Spectroscopy*, *Journal of Hazardous Materials*, *International Journal of Environmental Analytical Chemistry*, *Arabian Journal of Chemistry*, *Turkish Journal of Chemistry*, and *Journal of Nanostructure in Chemistry*. He has TUBITAK (Turkish Scientific and Technological Research Council) Encouragement Award in 2001. He is the recipient of the highest prestigious science award in Turkey, TUBITAK Science Award in 2020. He has also İlim Yayma Award from İlim Yayma Foundation in 2021. He has been a principal member of the Turkish Academy of Sciences (TUBA) since 2020. He has obtained a TÜBİTAK 2247-A National Fellowship for Outstanding Researchers (2021).

Corresponding Author

* M. Soylak

Email address: soylak@erciyes.edu.tr

Notes

The authors declare no competing financial interest.

ACKNOWLEDGMENTS

The authors thank the reviewers for the constructive comments for this work.

REFERENCES

1. M. A. Taher, M. Rahimi, and H. Fazelirad, *J. Lumin.*, 2014, **145**, 976–980. https://doi.org/10.1016/j.jlumin.2013.09.025
2. R. Dobrowolski, J. Dobrzyńska, and B. Gawrońska, *Environ Monit Assess.*, 2015, **187**, 1–8. https://doi.org/10.1007/s10661-014-4125-7
3. C. G. Magalhães, B. R. Nunes, M. B. O. Giacomelli, and J. B. B. da Silva, *J. Anal. At. Spectrom.*, 2003, **18**, 787–789. https://doi.org/10.1039/B302633G
4. S. Bodur, S. Erarpat, D. Selali Chormey, Ç. Büyükpınar, and S. Bakırdere, *Anal. Lett.*, 2019, 52, 539–549. https://doi.org/10.1080/00032719.2018.1477790
5. M. Sun and Q. Wu, *J. Hazard Mater.*, 2011, **192**, 935–939. https://doi.org/10.1016/j.jhazmat.2010.11.044
6. R. Pamphlett, M. Stoltenberg, J. Rungby, and G. Danscher, *Neurotoxicol. Teratol.*, 2000, **22**, 559–563. https://doi.org/10.1016/S0892-0362(00)00083-0
7. S. Moyano, R. G. Wuilloud, R. A. Olsina, J. A. Gásquez, and L. D. Martinez, *Talanta*, 2001, **54**, 211–219. https://doi.org/10.1016/S0039-9140(01)00310-1
8. Y. Yu, Q. Zhao, H. Bao, Q. Mou, Z. Shi, Y. Chen, and Y. Gao., *Geostand. Geoanal. Res.*, 2020, **44**, 617–627. https://doi.org/10.1111/ggr.12319
9. M. R. Jamali, J. M. Nakhaei, S. Sohrabnezhad, and R. Rahnama, *J. Anal. Chem.*, 2023, **78**, 980–987. https://doi.org/10.1134/S1061934823080075
10. P. V Racheva, N. P. Milcheva, F. Genc, and K. B. Gavazov, *Spectrochim. Acta A*, 2021, **262**, 120106. https://doi.org/10.1016/j.saa.2021.120106
11. V. A. Lemos, M. S. Santos, E. S. Santos, M. J. S. Santos, W. N. L. dos Santos, A. S. Souza, D. S. de Jesus, C. F. das Virgens, M. S. Carvalho, N. Oleszczuk, M. G. R. Vale, B. Welz, and S. L. C. Ferreira, *Spectrochim Acta B*, 2007, **62**, 4–12. https://doi.org/10.1016/j.sab.2006.12.006
12. S. Saracoglu, K. O. Saygi, O. D. Uluozlu, M. Tuzen, and M. Soylak, *Food Chem.*, 2006, **105**, 280–285. https://doi.org/10.1016/j.foodchem.2006.11.022
13. F. Tirpák, M. Halo, K. Tokárová, L. J. Binkowski, J. Vašíček, A. Svoradová, M. Błaszczyk-Altman, A. Kováčik, E. Tvrdá, P. Chrenek, N. Lukáč, and P. Massányi, *Life*, 2021, **11**, 1238. https://doi.org/10.3390/life11111238
14. J. Šoukal and S. Musil, *Microchem. J.*, 2022, **172**, 106963. https://doi.org/10.1016/j.microc.2021.106963
15. Z. Erbas, R. Maulana, E. Yilmaz, S. Ozdemir, E. Kilinc, and M. Soylak, *Int. J. Environ. Anal. Chem.*, 2020, **100**, 992–1003. https://doi.org/10.1080/03067319.2019.1646737
16. Z. M. Memon, E. Yilmaz, A. M. Shah, U. Sahin, T. G. Kazi, B. R. Devrajani, and M. Soylak, *Environ. Sci. Pollut. Res.*, 2017, **24**, 26513–26520. https://doi.org/10.1007/s11356-017-0236-3
17. Y. Lu, W. Zeng, J. Hu, and X. Hou, *Microchem. J.*, 2023, **195**, 109437. https://doi.org/10.1016/j.microc.2023.109437
18. M. F. Ayyıldız, D. N. Karaman, B. Kartoğlu, M. Şaylan, D. S. Chormey, and S. Bakırdere, *Food Chem.*, 2023, **429**, 136862. https://doi.org/10.1016/j.foodchem.2023.136862
19. N. Kolarova and P. Napiórkowski, *Ecohydrol. Hydrobiol.*, 2021, **21**, 655–668. https://doi.org/10.1016/j.ecohyd.2021.02.002
20. F. Uzcan and M. Soylak, *Chem. Pap.*, 2021, **75**, 6367–6375. https://doi.org/10.1007/s11696-021-01797-3
21. V. N. Bulut, Z. Bahadır, Ş. Ceylan, and M. Soylak, *Atom. Spectrosc.*, 2018, **39**, 46-54. https://doi.org/10.46770/AS.2018.01.006
22. F. Keskin, C. Sarikurkcu, I. Akata, and B. Tepe, *Environ. Sci. Pollut. Res.*, 2021, **28**, 36193–36204. https://doi.org/10.1007/s11356-021-13235-8
23. G. Saydan Kanberoglu, E. Yilmaz, and M. Soylak, *J. Iran. Chem. Soc.*, 2020, **17**, 1627–1634. https://doi.org/10.1007/s13738-020-01882-6
24. G. Baykal, D. Kazan, K. Seval, D. T. Bulut, S. G. Elci, U. Divrikli, and A. Akdogan, *Instrum. Sci. Technol.*, 2021, **50**, 288–305. https://doi.org/10.1080/10739149.2021.1996389

25. M. Soylak and R. Altin, *Atom. Spectrosc.*, 2014, **35**, 79–84. https://doi.org/10.46770/AS.2014.02.004
26. S. Pashaei, A. Hosseinzadeh, S. Mohammadi-Aghdam, Y. Saadat, and S. Hosseinzadeh, *Polym.-Plast. Tech. Mat.*, 2021, **60**, 994–1004. https://doi.org/10.1080/25740881.2021.1871625
27. X. Wang, J. I. Feng, Y. Bai, Q. Zhang, and Y. Yin, *Chem. Rev.*, 2016, **116**, 10983–11060. https://doi.org/10.1021/acs.chemrev.5b00731
28. J. Qi, X. Lai, J. Wang, H. Tang, H. Ren, Y. Yang, Q. Jin, L. Zhang, R. Yu, G. Ma, Z. Su, H. Zhaod, and D. Wang, *Chem. Soc. Rev.*, 2015, **44**, 6749–6773. https://doi.org/10.1039/C5CS00344J
29. S. Önel and G. Ergin, *J. Manuf. Sci. Eng.*, 2020, **142**, 74502. https://doi.org/10.1115/1.4046902
30. S. Abe, K. Fujii, and T. Sono, *Anal. Chim. Acta.*, 1994, **293**, 325–330. https://doi.org/10.1016/0003-2670(94)85038-0
31. M. Hosseini, N. Dalali, A. L. I. Karimi, and K. Dastanra, *Turk. J. Chem.*, 2010, **34**, 805–814. https://doi.org/10.3906/kim-1002-22
32. Z. Zang, Z. Hu, Z. Li, Q. He, and X. Chang, *J. Hazard. Mater.*, 2009, **172**, 958–963. https://doi.org/10.1016/j.jhazmat.2009.07.078
33. M. S. Jagirani, A. Balouch, S. A. Mahesar, A. Kumar, Abdullah, F. A. Mustafai, and M. I. Bhanger, *Polym. Bull.*, 2202, **77**, 5261–5279. https://doi.org/10.1007/s00289-019-03008-2
34. A. Kumara, A. Baloucha, A. A. Pathanb, Abdullaha, M. S. Jagirania, A. M. Mahara, M. Zubaira, B. Lagharia, *Acta Chemica Malaysia*, 2019, **3**, 1–15. https://doi.org/10.2478/acmy-2019-0001
35. K. S. Novoselov, A. K. Geim, S. V. Morozov, D. Jiang, Y. Zhang, S. V. Dubonos, I. V. Grigorieva, and A. A. Firsov, *Science*, 2004, **306**, 666–669. https://doi.org/10.1126/science.1102896
36. H. E. H. Ahmed, O. Ozalp, and M. Soylak, *J. Food Compost. Anal.*, 2023, **118**, 105163. https://doi.org/10.1016/j.jfca.2023.105163
37. Z. Shi, Q. Zhao, B. Guo, T. Ji, and H. Wang, *Mater. Des.*, 2020, **193**, 108858. https://doi.org/10.1016/j.matdes.2020.108858
38. J.-J. Fan, S.-Y. Shen, Y. Chen, L.-N. Wu, J. Peng, X.-X. Peng, C.-G. Shi, L. Huang, W.-F. Lin, and S.-G. Sun, *Electrochem. Commun.*, 2018, **90**, 16–20. https://doi.org/10.1016/j.elecom.2018.03.004
39. X. C. Wu, Y. R. Tao, Z. J. Han, and B. D. Zhang, *J. Mater. Chem.*, 2003, **13**, 2649–2651. https://doi.org/10.1039/B305924C
40. M. K. Rasmussen, S. A. Foster, F. C. Filippo, B. Hinnemann, S. Helveg, K. Meinander, F. Besenbacher, and V. J. Lauritsen, *Phys. Rev. B*, 2011, **84**, 235419. https://doi.org/10.1103/PhysRevB.84.235419.
41. C. Long, X. Li, Z. Jiang, P. Zhang, Z. Qing, T. Qing, B. Feng, *J. Hazard. Mater.*, 2021, **413**, 125470. https://doi.org/10.1016/j.jhazmat.2021.125470
42. N. T. Shelke and D. J. Late, *Sens. Actuators A Phys.*, 2019, **295**, 160–168. https://doi.org/10.1016/j.sna.2019.05.045
43. S. Demirel, M. Tuzen, S. Saracoglu, and M. Soylak, *J. Hazard. Mater.*, 2008, **152**, 1020–1026. https://doi.org/10.1016/j.jhazmat.2007.07.077
44. R. Dalipi, E. Marguí, L. Borgese, and L. E. Depero, *Food Chem.*, 2017, **218**, 348–355, https://doi.org/10.1016/j.foodchem.2016.09.022
45. M. Y. Nassar, I. S. Ahmed, and I. Samir, *Spectrochim. Acta A*, 2014, **131**, 329–334. https://doi.org/10.1016/j.saa.2014.04.040
46. R. Hajavazzade, A. R. Mahjoub, and M. Kargarrazi, *Res. Chem. Intermediat.*, 2019, **45**, 2341–2355. https://doi.org/10.1007/s11164-019-03737-z
47. F. Shajarat, K. Ghanemi, M. Alimoradi, and M. Ramezani, *Int. J. Environ. Anal. Chem.*, 2023, **103**, 5010–5024. https://doi.org/10.1080/03067319.2021.1933962
48. T. Padma, D. K. Gara, A. N. Reddy, S. V. P. Vattikuti, and C. M. Julien, *Nanomaterials*, 2022, **12**, 1160. https://doi.org/10.3390/nano12071160
49. J. Zhang, W. Kang, M. Jiang, Y. You, Y. Cao, T.-W. Ng, D. Y. W. Yu, C.-S. Lee, and J. Xu, *Nanoscale*, 2017, **9**, 1484–1490. https://doi.org/10.1039/C6NR09166K
50. L. Zhang, L. Sun, Y. Huang, Y. Sun, T. Hu, K. Xu, and F. Ma, *J. Mater. Sci.*, 2017, **52**, 13561–13571. https://doi.org/10.1007/s10853-017-1417-7
51. B. Kartoğlu, A. Bahçivan, S. Erarpat, A. Bayraktar, and S. Bakirdere, *J. Food Compost. Anal.*, 2023, **121**, 105373. https://doi.org/10.1016/j.jfca.2023.105373
52. R. M. Smith and A. E. Martell, Critical Stability Constants: Second Supplement, Volume 6, Springer Science & Business Media, 1989. https://link.springer.com/book/10.1007/978-1-4615-6764-6
53. H. E. H. Ahmed, A. M. A. Mohammed, and M. Soylak, *Food Chem.*, 2023, **428**, 136794. https://doi.org/10.1016/j.foodchem.2023.136794
54. A. S. Amin, M. Y. Nassar, and A. Gomaa, *Int. J. Environ. Anal. Chem.*, 2023, **103**, 1550–1571. https://doi.org/10.1080/03067319.2021.1877281
55. A. Duran, M. Tuzen, and M. Soylak, *J. Hazard. Mater.*, 2009, **169**, 466–471. https://doi.org/10.1016/j.jhazmat.2009.03.119
56. Y. Yamini, M. Chaloosi, and H. Ebrahimzadeh, *Talanta*, 2002, **56**, 797–803. https://doi.org/10.1016/S0039-9140(01)00615-4
57. A. Sabarudin, O. Noguchi, M. Oshima, K. Higuchi, and S. Motomizu, *Microchim. Acta*, 2007, **159**, 341–348. https://doi.org/10.1007/s00604-007-0734-y
58. M. Soylak, L. Elci, and M. Dogan, *J. Trace Microprobe Tech.*, 1999, **17**, 149–156. https://webofscience.clarivate.cn/wos/woscc/full-record/WOS:000080056100001
59. A. Poudel, S. Adhikari, T. Y. Asfaha, J. G. Lawrence, M. M. Kandage, M. Marszewski, and J. R. Kirchhoff, *Resour. Conserv. Recycl.*, 2023, **199**, 107199. https://doi.org/10.1016/j.resconrec.2023.107199.
60. M. Ghaedi, F. N. Azad, K. Dashtian, S. Hajati, A. Goudarzi, and M. Soylak, *Spectrochim. Acta A*, 2016, **167**, 157–164. https://doi.org/10.1016/j.saa.2016.05.025
61. V. Eyupoglu and A. Unal, *J. Environ. Chem. Eng.*, 2023, **11**, 110570. https://doi.org/10.1016/j.jece.2023.110570.
62. Y. E. Unsal, M. Tuzen, and M. Soylak, *J. AOAC Int.*, 2016, **99**, 534–538. https://doi.org/10.5740/jaoacint.11-0490
63. V. H. Thien, and N. V. Dong, *Vietnam J. Chem.*, 2023, **61(S2)**, 66–72. https://doi.org/10.1002/vjch.202300063
64. A.U. Karatepe, M. Soylak, and L. Elci, *Anal. Lett.*, 2003, **36**, 797–812. https://doi.org/10.1081/AL-120018800
65. H. Ashkenani and M. A. Taher, *Int. J. Environ. Anal. Chem.*, 2013, **93**, 1132–1145. https://doi.org/10.1080/03067319.2012.708746
66. M. A. Taher, E. Rezaeipour, and D. Afzali, *Talanta*, 2004, **63**, 797–801. https://doi.org/10.1016/j.talanta.2003.12.017
67. Y. Bakircioglu, D. Bakircioglu, and S. Akman, *J. Trace Microprobe Tech.*, 2003, 21, 467–478. https://doi.org/10.1081/TMA-120023063
68. L. Elci, M. Soylak, A. Uzun, E. Büyükpatır, and M. Doğan, *Fresenius J. Anal. Chem.*, 2000, **368**, 358–361. https://doi.org/10.1007/s002160000448
69. K. Hu, P. Li, S. Yang, and X. Wen, *J. Anal. At. Spectrom.*, 2020, **35**, 526–533. https://doi.org/10.1039/C9JA00436J